JACS
JOURNAL OF THE AMERICAN CHEMICAL SOCIETY

ARTICLE

pubs.acs.org/JACS

Formic Acid Catalyzed Hydrolysis of SO_3 in the Gas Phase: A Barrierless Mechanism for Sulfuric Acid Production of Potential Atmospheric Importance

Montu K. Hazra and Amitabha Sinha*

Department of Chemistry and Biochemistry, University of California, San Diego, La Jolla, California 92093-0314, United States

Supporting Information

ABSTRACT: Computational studies at the B3LYP/6-311++G-(3df,3pd) and MP2/6-311++G(3df,3pd) levels are performed to explore the changes in reaction barrier height for the gas phase hydrolysis of SO_3 to form H_2SO_4 in the presence of a single formic acid (FA) molecule. For comparison, we have also performed calculations for the reference reaction involving water assisted hydrolysis of SO_3 at the same level. Our results show that the FA assisted hydrolysis of SO_3 to form H_2SO_4 is effectively a barrierless process. The barrier heights for the isomerization of the $SO_3\cdots H_2O\cdots FA$ prereactive collision complex, which is the rate limiting step in the FA assisted hydrolysis, are found to be respectively 0.59 and 0.08 kcal/mol at the B3LYP/6-311++G-(3df,3pd) and MP2/6-311++G(3df,3pd) levels. This is substantially lower than the ~7 kcal/mol barrier for the corresponding step in the hydrolysis of SO_3 by two water molecules—which is currently the accepted mechanism for atmospheric sulfuric acid production. Simple kinetic analysis of the relative rates suggests that the reduction in barrier height facilitated by FA, combined with the greater stability of the prereactive $SO_3\cdots H_2O\cdots FA$ collision complex compared to $SO_3\cdots H_2O\cdots H_2O$ and the rather plentiful atmospheric abundance of FA, makes the formic acid mediated hydrolysis reaction a potentially important pathway for atmospheric sulfuric acid production.

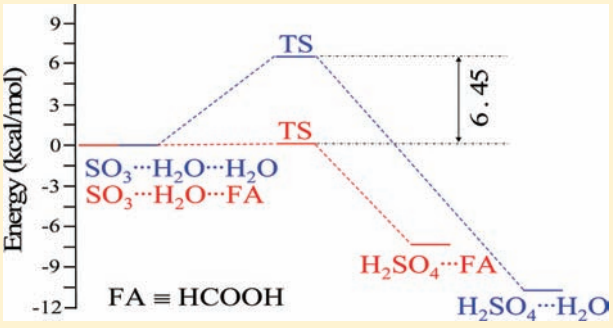

1. INTRODUCTION

Sulfuric acid (H_2SO_4) is an important contributor to acid rain[1−3] and is known to influence atmospheric nucleation proceses.[4−10] The microscopic particles suspended in Earth's atmosphere, known as aerosols, play an important role in degrading visibility, promoting atmospheric heterogeneous chemistry, as well as negatively impacting human health.[11−14] Aerosol particles also have the potential to influence climate by absorbing and reflecting solar radiation and modifying cloud formation.[15−20] Because of its importance, there have been many studies investigating the physical, photochemical, and spectroscopic properties of sulfuric acid.[21−37] The reaction of sulfur trioxide (SO_3) with water vapor is believed to be the principal mechanism for gas phase sulfuric acid (H_2SO_4) formation in the atmosphere.[2,38−40] As a result, this reaction has received much attention in the scientific literature both experimentally[39−51] and theoretically.[52−63] Initially, the 1:1 $SO_3\cdots H_2O$ complex, formed from the addition of one SO_3 molecule to one H_2O molecule, as shown below in reactions 1 and 2, was thought to be involved in the production of H_2SO_4.[42,52]

$$SO_3 + H_2O + M \rightleftharpoons SO_3\cdots H_2O + M \quad (1)$$

$$SO_3\cdots H_2O \rightarrow H_2SO_4 \quad (2)$$

Subsequent theoretical calculations, however, revealed that this mechanism, involving a four-member ring transition state, has a large activation energy barrier (~28 to 32 kcal/mol)[53−56] and consequently was not favored as a possible route for atmospheric H_2SO_4 production (see Figure 1).[54,56] Theoretical calculations also showed that the introduction of a second water molecule in the gas phase SO_3 hydrolysis reaction substantially reduces the activation barrier through the formation ~of a six-member ring transition state (see Figure 1).[55] The rate limiting step for H_2SO_4 formation via this mechanism involves the unimolecular isomerization of the prereactive $SO_3\cdots H_2O\cdots H_2O$ collision complex to form $H_2SO_4\cdots$ H2O, and various calculations have estimated the barrier height associated with this step to be in the range between ~6.6−13 kcal/mol.[62,55,56,58,59] The presence of additional water molecules has been shown to further reduce the barrier height for the hydrolysis reaction, with four or more water molecules effectively removing the barrier completely.[58,51] Consistent with these theoretical findings, experimental work has shown that the gas-phase SO_3 hydrolysis reaction is second order with respect to the partial pressure of water and exhibits a strong negative temperature dependence.[40,49,50] The second order dependence on water

Received: August 5, 2011
Published: September 20, 2011

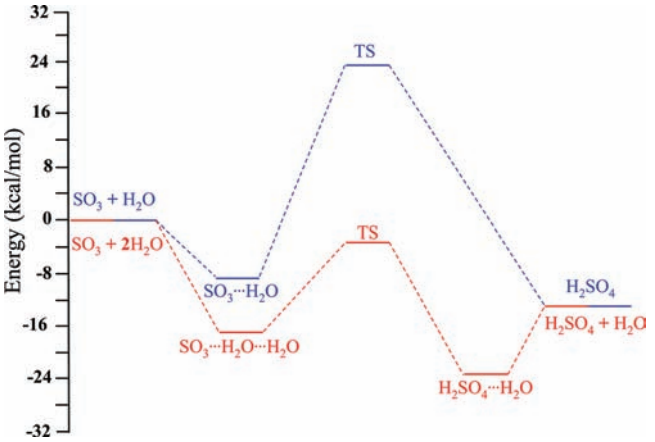

Figure 1. Potential energy profiles for the gas phase hydrolysis of SO_3 involving: (a) one water molecule (blue): $SO_3\cdots H_2O \rightarrow H_2SO_4$ and (b) two water molecules (red): $SO_3\cdots H_2O\cdots H_2O \rightarrow H_2SO_4\cdots H_2O$. In both cases unimolecular isomerization of a prereactive collision complex is the rate determining step. The energetics in the figure is adapted from the calculations given in ref 55.

concentration is consistent with two potential pathways for SO_3 hydrolysis, with one pathway involving the collision of an $SO_3\cdots H_2O$ complex with a H_2O molecule (reaction 3) and the other involving a SO_3 molecule colliding with a water dimer ($H_2O\cdots H_2O$) (reaction 4).

$$SO_3\cdots H_2O + H_2O \rightleftharpoons SO_3\cdots H_2O\cdots H_2O \rightarrow H_2SO_4\cdots H_2O \quad (3)$$

$$SO_3 + H_2O\cdots H_2O \rightleftharpoons SO_3\cdots H_2O\cdots H_2O \rightarrow H_2SO_4\cdots H_2O \quad (4)$$

In either case, the result of the bimolecular encounter is the formation of an $SO_3\cdots H_2O\cdots H_2O$ prereactive collision complex which then isomerizes into $H_2SO_4\cdots H_2O$ through a common transition state.[55,59] While the greater stability of the $SO_3\cdots H_2O + H_2O$ reactants over $SO_3 + H_2O\cdots H_2O$ appears to favor the pathway associated with reaction 3, this gain is countered by the fact that the pathway associated with reaction 3 has reduced available energy for overcoming the isomerization barrier. Thus, both pathways (reactions 3 and 4) are expected to be important,[40,50,59,61] although to the best of our knowledge there has been no prior analysis in the literature addressing whether one of the pathways dominates over the other.

Given that a second water molecule considerably reduces the activation energy for gas phase SO_3 hydrolysis, it is natural to inquire if other atmospheric molecules can also be effective in lowering the reaction barrier. Recent work, for example, has shown that HO_2 radicals can significantly reduce the barrier height for the SO_3 hydrolysis reaction.[64] However, given the low concentration of HO_2 in the atmosphere, HO_2 radical catalyzed hydrolysis will likely not be competitive with the original mechanism involving water catalysis. In this article, we investigate a new mechanism for SO_3 hydrolysis that is catalyzed by formic acid. We note that the atmospheric concentration of formic acid (FA) is relatively large[65−71] and that the ability of FA to lower the barriers for gas phase unimolecular isomerization reactions involving hydrogen atom transfer has recently been demonstrated for several systems, including model biological molecules,[72,73] atmospheric radicals,[74] keto−enol tautomerization of vinyl alcohol,[75] as well as organic multicomponent reactions.[76] Below we show that a single FA molecule can also effectively eliminate the barrier for the SO_3 hydrolysis reaction to form sulfuric acid. Specifically, we provide evidence that, analogous to the situation involving water catalysis, FA can participate in the atmospheric hydrolysis of SO_3 either by directly colliding with a $SO_3\cdots H_2O$ complex (reaction 5) and/or by having an SO_3 molecule collide with a $FA\cdots H_2O$ complex (reaction 6). In both cases, the prereactive $SO_3\cdots H_2O\cdots FA$ collision complex is formed.

$$SO_3\cdots H_2O + FA \rightleftharpoons SO_3\cdots H_2O\cdots FA \rightarrow H_2SO_4\cdots FA \quad (5)$$

$$SO_3 + H_2O\cdots FA \rightleftharpoons SO_3\cdots H_2O\cdots FA \rightarrow H_2SO_4\cdots FA \quad (6)$$

Once formed, the $SO_3\cdots H_2O\cdots FA$ prereactive collision complex can subsequently undergo unimolecular isomerization to produce $H_2SO_4\cdots FA$. Thus, while in the water assisted SO_3 hydrolysis the rate determining step involves isomerization of the $SO_3\cdots H_2O\cdots H_2O$ collision complex, for the FA catalyzed reaction the analogous step involves isomerization of the $SO_3\cdots H_2O\cdots FA$ complex. On the basis of the calculation presented below, we demonstrate that the unimolecular isomerization of $SO_3\cdots H_2O\cdots FA$ to form $H_2SO_4\cdots FA$ is effectively a barrierless process and that the overall rate for the hydrolysis reaction is independent of whether the $SO_3\cdots H_2O\cdots FA$ complex is formed via the $SO_3\cdots H_2O$ + FA or SO_3 + $FA\cdots H_2O$ pathways. We further show that, given the relatively high concentration of formic acid (FA) in the atmosphere, the yield of H_2SO_4 from FA catalyzed hydrolysis of SO_3 is competitive with and may even surpass that from the currently accepted mechanism involving water catalysis. Given the importance of sulfuric acid in atmospheric aerosol formation, this new mechanism for SO_3 hydrolysis can potentially impact our fundamental understanding of how "critical nuclei", required for the initial stages of aerosol growth, are generated in the atmosphere.

2. COMPUTATIONAL METHOD

The Gaussian-03 suite of programs[77] has been used to carry out all the quantum chemistry calculations presented here. The calculations have been performed using both MP2 and density functional theory (DFT). For the DFT calculations, the popular Becke's three parameter hybrid functional in conjunction with the Lee−Yang−Parr correlation (B3LYP) has been used.[78,79] Initial starting geometries for the monomers and 1:1 hydrogen-bonded (H-bonded) and ternary H-bonded complexes involved in the FA assisted hydrolysis reaction as reported in Table 1 of the Supporting Information have been optimized at the MP2 level using the 6-31G(d,p) basis set. In the case of the water assisted hydrolysis reaction, initial calculations were performed at the B3LYP/6-31+G(d) level to reproduce the barrier height reported by Loerting et al. at this same level of theory (see below).[59] Transition states for both the water and FA assisted reactions have been located using the QST2/QST3 routine in Gaussian-03. Furthermore, in the case of the FA assisted unimolecular isomerization, an intrinsic reaction coordinate (IRC) calculation was also performed at the MP2/6-31G(d,p) level to unambiguously verify the location of the transition state connecting the reactant and product. Since the binding energy of the $SO_3\cdots H_2O$ complex and the energy barrier for the $SO_3\cdots H_2O\cdots H_2O \rightarrow H_2SO_4\cdots H_2O$ unimolecular isomerization are rather sensitive to the size of the basis set,[62,63] the MP2/6-31G(d,p) or B3LYP/6-31+G(d)

Table 1. A Few Selected Bond Lengths (angstroms) for the $SO_3\cdots H_2O\cdots FA$, TS, and $H_2SO_4\cdots FA$ Complexes Predicted at the B3LYP/6-311++G(3df,3pd) and MP2/6-311++G(3df,3pd) Levels of Calculations[a]

	B3LYP/6-311++G(3df,3pd)			MP 2/6-311++G(3df,3pd)		
geometrical parameters	$SO_3\cdots H_2O\cdots FA$	TS	$H_2SO_4\cdots FA$	$SO_3\cdots H_2O\cdots FA$	TS	$H_2SO_4\cdots FA$
$S_1\cdots O_2$	2.037	1.800	1.634	1.994	1.782	1.621
$O_2\cdots O_4$	2.605	2.416	2.881	2.578	2.401	2.852
O_4—H_3	1.598	1.183	0.980	1.571	1.187	0.977
$O_8\cdots O_6$	2.710	2.490	2.644	2.678	2.481	2.620
O_8—H_7	1.722	1.438	1.003	1.690	1.435	1.000
O_2—H_3	1.008	1.234	1.902	1.008	1.216	1.875
C_5═O_4	1.218	1.249	1.317	1.222	1.250	1.317
C_5—O_6	1.307	1.27	1.212	1.306	1.272	1.216
O_6—H_7	0.991	1.054	1.646	0.990	1.048	1.623
S_1—O_8	1.445	1.473	1.557	1.447	1.471	1.550
$S_1\cdots C_5$	4.171	3.844	3.979	3.996	3.711	3.865

[a] See Figure 2 for atom numberings of the $SO_3\cdots H_2O\cdots FA$, TS, and $H_2SO_4\cdots FA$ complexes.

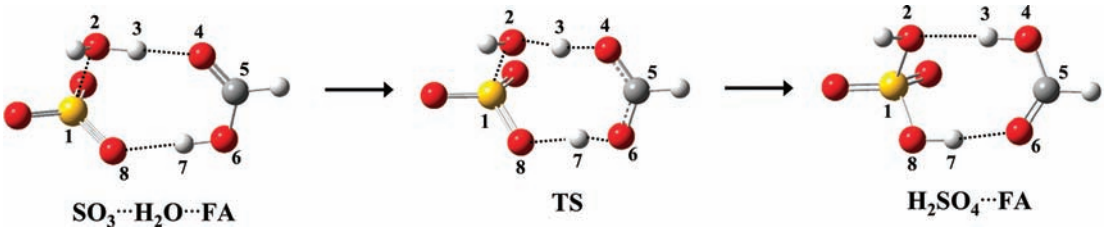

Figure 2. The MP2/6-311++G(3df,3pd) level optimized geometries of the $SO_3\cdots H_2O\cdots FA$ (FA ≡ formic acid) and $H_2SO_4\cdots FA$ complexes as well as the transition state (TS) for the $SO_3\cdots H_2O\cdots FA \rightarrow H_2SO_4\cdots FA$ unimolecular isomerization reaction.

level predicted geometries, including that of the transition states, were further optimized using the larger 6-311++G(3df,3pd) basis set. Furthermore, geometry optimizations using the larger basis set are also required to reduce the basis set superposition error (BSSE), even though full (100%) counterpoise corrections often underestimate binding energies of dimeric complexes.[80−82] Except for the calculations carried out at the MP2/6-311++G(3df,3pd) level, normal-mode frequency analysis has been performed for all geometries optimized at the other levels of calculations to verify that the stable minima have all positive frequencies and that the transition state (TS) geometries have only one imaginary frequency (see Table 1 of the Supporting Information). The normal-mode frequencies of the reactant, product, and TS were also used to estimate the zero-point vibrational energy corrections associated with the isomerization reaction barrier heights, binding energies, and relative stabilities of the various species. In the case of the MP2/6-311++G(3df,3pd) level calculations, the B3LYP/6-311++G(3df,3pd) level predicted frequencies were used to estimate the corresponding zero point vibrational energy corrections.

3. RESULTS AND DISCUSSION

3A. Computational Results. For the FA catalyzed reaction, the MP2/6-311++G(3df,3pd) level optimized geometries of $SO_3\cdots H_2O\cdots FA$, $H_2SO_4\cdots FA$, and the TS associated with the $SO_3\cdots H_2O\cdots FA \rightarrow H_2SO_4\cdots FA$ unimolecular isomerization reaction are shown in Figure 2. A few selected bond lengths predicted at both the B3LYP/6-311++G(3df,3pd) and MP2/6-311++G(3df,3pd) levels for the $SO_3\cdots H_2O\cdots FA$ and $H_2SO_4\cdots FA$ complexes as well as the TS are given in Table 1. The optimized geometries of these species are given in the Supporting Information. From Table 1, it is seen that the intermolecular distances between the SO_3, H_2O, and FA subunits at the TS are shorter than the corresponding distances in the prereactive $SO_3\cdots H_2O\cdots FA$ collision complex. For example, at the MP2/6-311++G(3df,3pd) level, the $S_1\cdots O_2$ and $S_1\cdots C_5$ distances are shortened respectively from their values of 1.994 Å and 3.996 Å in the $SO_3\cdots H_2O\cdots FA$ complex to 1.782 Å and 3.711 Å in the TS. Looking at Figure 2, we see that in going from the $SO_3\cdots H_2O\cdots FA$ collision complex to the product $H_2SO_4\cdots FA$ complex, the C−O single bond of the H−O−C subunit in FA is converted to a C═O double bond as the hydrogen atom is transferred to SO_3, and in step with this transformation, the O═C double bond of the FA moiety becomes a single bond upon accepting the hydrogen atom from H_2O. Also, in going from the $SO_3\cdots H_2O\cdots FA$ collision complex to the TS, the hydrogen bonded O−H distances in both the H_2O and FA subunits are elongated. At the MP2/6-311++G(3df,3pd) level, the O_2—H_3 bond distance in the H_2O subunit and the O_6—H_7 bond distance of the FA subunit are elongated from their respective values of 1.008 and 0.990 Å in the $SO_3\cdots H_2O\cdots FA$ collision complex to 1.216 and 1.048 Å at the TS.

Figure 3 shows a schematic of the corresponding potential energy profile for the FA assisted SO_3 hydrolysis reaction. Basically, there are two main pathways through which the FA assisted hydrolysis of SO_3 can take place. It can occur either via the bimolecular encounter involving an $SO_3\cdots H_2O$ complex hitting FA (i.e., $SO_3\cdots H_2O$ + FA) or through the collision between SO_3 and a $FA\cdots H_2O$ complex (i.e., SO_3 + $FA\cdots H_2O$). Both encounters produce the same $SO_3\cdots H_2O\cdots FA$ collision

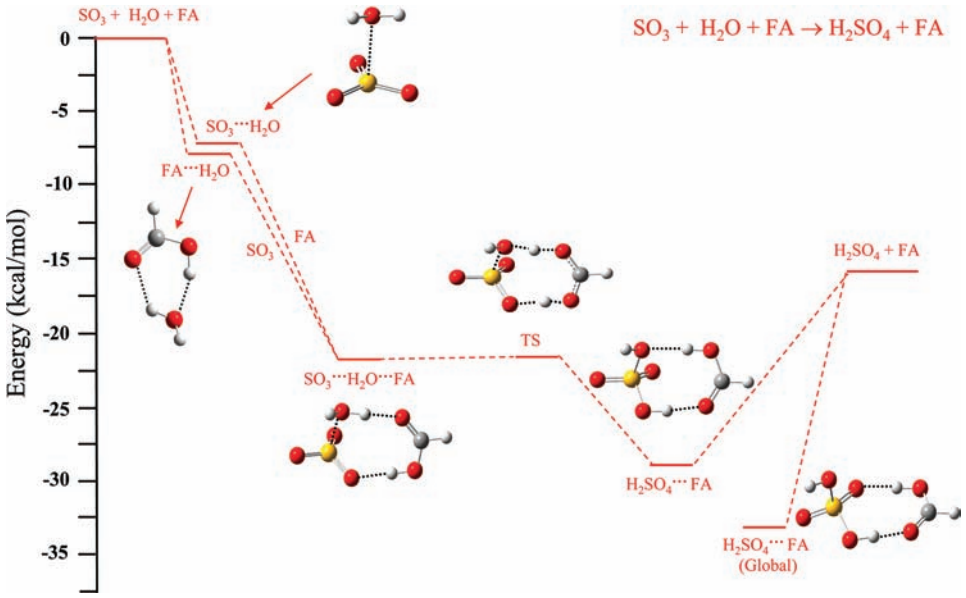

Figure 3. Potential energy profile for the $SO_3 + H_2O + FA \rightarrow H_2SO_4 + FA$ reaction. The energy profile has been calculated at the MP2/6-311++G(3df,3pd) level and includes zero point vibrational energy corrections at the B3LYP/6-311++G(3df,3pd) level. The combined energy of the isolated monomers in the reactant side has been taken as zero at infinite separation.

Table 2. Zero Point Vibrational Energy (ZPE) Uncorrected and Corrected Barrier Heights (kcal/mol) for the $SO_3\cdots H_2O\cdots FA \rightarrow H_2SO_4\cdots FA$ and $SO_3\cdots H_2O\cdots H_2O \rightarrow H_2SO_4\cdots H_2O$ Unimolecular Isomerization Reactions at Different Levels of Calculations

	$SO_3\cdots H_2O\cdots FA \rightarrow H_2SO_4\cdots FA$		$SO_3\cdots H_2O\cdots H_2O \rightarrow H_2SO_4\cdots H_2O$	
level of calculations	ZPE uncorrected	ZPE corrected	ZPE uncorrected	ZPE corrected
MP 2/6-31G(d,p)	5.06	2.62		
B3LYP/6-311++G(3df,3pd)	3.08	0.59	8.43	7.05
MP 2/6-311++G(3df,3pd)	2.57	0.08	7.90	6.53

complex. As we discuss further below, on energetic grounds, the rates for H_2SO_4 formation via both these pathways are expected to be similar. We note that although the $SO_3\cdots H_2O\cdots FA$ complex can also be formed through a ternary collision involving the simultaneous collision of isolated SO_3, H_2O, and FA molecules, the probability of this three-body collision occurring is expected to be relatively low. The relative energies shown in Figure 3 are based on calculations at the MP2/6-311++G(3df,3pd) level and include zero point vibrational energy corrections. The barrier heights and binding energies predicted for this reaction at the MP2/6-31G(d,p), B3LYP/6-311++G(3df,3pd), and MP2/6-311++G(3df,3pd) levels are summarized in Tables 2 and 3. From Table 2 it is seen that at the MP2/6-31G(d,p) level the zero point corrected barrier height for the rate limiting step involving unimolecular isomerization of the collision complex, $SO_3\cdots H_2O\cdots FA \rightarrow H_2SO_4\cdots FA$, is 2.62 kcal/mol. The predicted value for this barrier height is lowered when using the larger 6-311++G(3df,3pd) basis set, and we find that for both the B3LYP and MP2 methods this larger basis set gives zero point vibrational energy corrected barrier heights that are respectively only 0.59 and 0.08 kcal/mol. Therefore, with formic acid, the barrier associated with the rate limiting step effectively becomes negligible, and hence, sulfuric acid formation through FA catalyzed hydrolysis of SO_3 is expected to be facile. Looking at Figure 3, we also see that there are two energetically distinct structures associated with the $H_2SO_4\cdots FA$ complex in the exit channel. Frequency analyses at both the MP2/6-31G(d,p) and B3LYP/6-311++G(3df,3pd) levels confirm that these two stationary points are true minima, as reflected by their complete sets of positive frequencies. One structure corresponds to the global minimum and the other to a local minimum of the $H_2SO_4\cdots FA$ complex. In the global minimum structure, the S═O and OH groups of the H_2SO_4 unit act respectively as hydrogen acceptor and donor, whereas in the local minimum structure two OH groups of the H_2SO_4 unit are involved in hydrogen-bond formation with FA. The $H_2SO_4\cdots FA$ local minimum structure, shown more clearly in Figure 2, corresponds to the end point of the intrinsic reaction coordinate calculation, which connects it with the $SO_3\cdots H_2O\cdots FA$ prereactive collision complex via the TS.

Another aspect of the potential energy curve shown in Figure 3 that is worth mentioning is the ability of both the $SO_3\cdots H_2O$ + FA and SO_3 + $FA\cdots H_2O$ pathways to form the same $SO_3\cdots H_2O\cdots FA$ prereactive collision complex. At the MP2/6-311++G(3df,3pd) level, the zero point corrected binding energy difference between the $SO_3\cdots H_2O$ and $FA\cdots H_2O$ reactant complexes is only 0.74 kcal/mol in favor of $FA\cdots H_2O$ (see Table 3 and Figure 3). As can be seen in Figure 3, the structure of the $SO_3\cdots H_2O$ fragment in the $SO_3\cdots H_2O\cdots FA$ prereactive collision complex is similar to the equilibrium structure of the isolated $SO_3\cdots H_2O$ reactant complex. Thus, when the $SO_3\cdots H_2O\cdots FA$ collision complex is formed via the $SO_3\cdots H_2O$ + FA bimolecular encounter, very little reorientation of the H_2O subunit in the $SO_3\cdots H_2O$ reactant is required to produce the $SO_3\cdots H_2O\cdots FA$ prereactive collision complex. By contrast, for the SO_3 + $FA\cdots H_2O$ pathway, we find that the structure of the $FA\cdots H_2O$ moiety in the $SO_3\cdots H_2O\cdots FA$ prereactive

dx.doi.org/10.1021/ja207393v |J. Am. Chem. Soc. 2011, 133, 17444–17453

Table 3. Zero Point Vibrational Energy (ZPE) Uncorrected and Corrected Binding Energies (kcal/mol) of All 1:1 Dimeric and 1:1:1 Ternary Hydrogen-Bonded (H-Bonded) Complexes at Different Levels of Calculations[a]

	MP 2/6-31G(d,p)		B3LYP/6-311++G(3df,3pd)		MP 2/6-311++G(3df,3pd)	
molecular complexes	ZPE uncorrected	ZPE corrected	ZPE uncorrected	ZPE corrected	ZPE uncorrected	ZPE corrected
$SO_3\cdots H_2O$	12.26	10.15	8.36	6.23	9.38	7.25
$FA\cdots H_2O$	13.90	11.01	9.58	7.04	10.53	7.99
$SO_3\cdots H_2O\cdots FA$	28.76	24.02	23.41	18.78	26.32	21.69
$H_2SO_4\cdots FA$ (local)	15.66	13.95	11.66	10.01	14.62	12.97
$H_2SO_4\cdots FA$ (global)	19.00	17.30	16.49	15.01	18.87	17.39
$H_2O\cdots H_2O$	7.05	4.8	4.83	2.66	5.30	3.14
$SO_3\cdots H_2O\cdots H_2O$			19.10	13.94	21.30	16.14
$H_2SO_4\cdots H_2O$			11.55	9.26	13.21	10.92

[a] The binding energy for a particular binary or ternary H-bonded complex has been calculated by subtracting the total electronic energies of monomers forming the complex from the calculated energies of that complex. The calculated electronic energies for monomers and complexes are given in Table 1 of the Supporting Information.

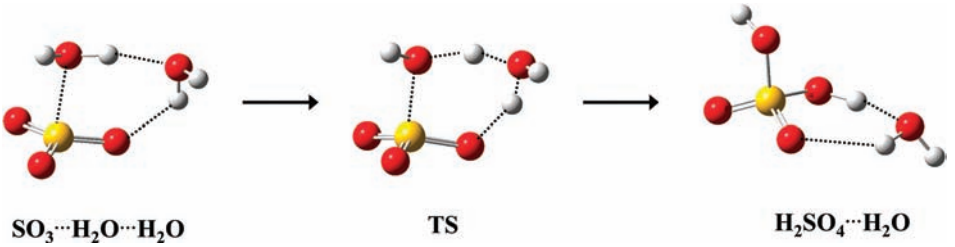

Figure 4. MP2/6-311++G(3df,3pd) level optimized geometries of $SO_3\cdots H_2O\cdots H_2O$, $H_2SO_4\cdots H_2O$, and TS for the $SO_3\cdots H_2O\cdots H_2O \rightarrow H_2SO_4\cdots H_2O$ unimolecular isomerization reaction.

collision complex is a bit more distorted compared to the equilibrium structure found in the isolated $FA\cdots H_2O$ reactant. The optimized geometry of the $FA\cdots H_2O$ complex is given in Figure 3. Thus, in producing the $SO_3\cdots H_2O\cdots FA$ prereactive collision complex via the SO_3 + $FA\cdots H_2O$ pathway, one expects that some reorientation of the H_2O subunit in the $FA\cdots H_2O$ reactant will be required as it approaches SO_3. In order to confirm that the SO_3 + $FA\cdots H_2O$ channel proceeds through the same minimum energy $SO_3\cdots H_2O\cdots FA$ collision complex as that found for the $SO_3\cdots H_2O$ + FA channel, we have carried out several diagnostic calculations at the MP2/6-31G(d,p) level in which we performed geometry optimization of the prereactive collision complex arising from a number of different starting geometries for the SO_3 + $FA\cdots H_2O$ reactants as well as distorted configurations of the $SO_3\cdots H_2O\cdots FA$ collision complex. For the SO_3 + $FA\cdots H_2O$ reactants, the trial geometries were such that the water subunit points toward the SO_3, as required for initiating the hydrolysis reaction. Examples of two such initial trial geometries used in examining the formation of the $SO_3\cdots H_2O\cdots FA$ collision complex are given in the Supporting Information. These diagnostic calculations basically confirm that the minimum energy path for both the SO_3 + $FA\cdots H_2O$ and $SO_3\cdots H_2O$ + FA channels involves formation of the same $SO_3\cdots H_2O\cdots FA$ collision complex. We find that all starting reactant geometries and/or distorted $SO_3\cdots H_2O\cdots FA$ configurations eventually end up giving the same minimum energy $SO_3\cdots H_2O\cdots FA$ prereactive collision complex configuration: the one given in Figure 2.

In order to compare the FA assisted and water assisted hydrolysis reactions on an equal footing, we have also performed a similar set of calculations for the SO_3 hydrolysis reaction involving two water molecules. The MP2/6-311++G(3df,3pd) level optimized geometries for the $SO_3\cdots H_2O\cdots H_2O$ and $H_2SO_4\cdots H_2O$ complexes, as well as the TS associated with the rate limiting $SO_3\cdots H_2O\cdots H_2O \rightarrow H_2SO_4\cdots H_2O$ unimolecular isomerization reaction for this reference reaction, are shown in Figure 4. The barrier heights and binding energies predicted at the various levels of calculations, including the MP2/6-311++G(3df,3pd) level, are summarized in Tables 2 and 3. In Figure 5 the zero point energy corrected potential energy diagram for the water assisted hydrolysis reaction predicted at the MP2/6-311++G(3df,3pd) level is shown. In the entrance channel we see the two bimolecular collisional pathways associated with the SO_3 + $H_2O\cdots H_2O$ and $SO_3\cdots H_2O$ + H_2O channels that can form the $SO_3\cdots H_2O\cdots H_2O$ prereactive collision complex. Further to the right, the TS and product $H_2SO_4\cdots H_2O$ complex are also shown in Figure 5. As the water catalyzed hydrolysis reaction has already been studied extensively by several groups, we next compare our results for this reference reaction with those from the earlier studies. We performed the B3LYP/6-31+G(d) level calculations for the hydrolysis of SO_3 by two water molecules in order to reproduce the barrier height reported previously by Loerting et al.[59,60] at the same level. Our calculation at the B3LYP/6-31+G(d) level predicts the zero point uncorrected barrier height for the unimolecular isomerization of the $SO_3\cdots H_2O\cdots H_2O$ complex to be 10.04 kcal/mol, which is only 0.01 kcal/mol higher than the value (10.03 kcal/mol) reported by Loerting et al.[59] Furthermore, to verify the location of the TS, we also compared our calculated electronic energy and imaginary frequency for the TS, computed at the B3LYP/6-311++G(3df,3pd)

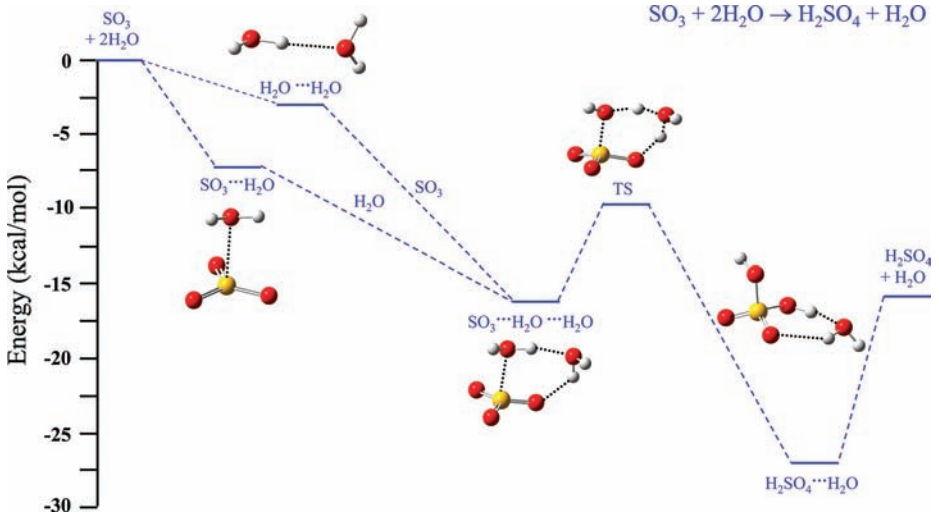

Figure 5. Potential energy profile for the $SO_3 + 2H_2O \rightarrow H_2SO_4 + H_2O$ reaction. The energy profile has been calculated at the MP2/6-311++G(3df,3pd) level and includes zero point vibrational energy corrections at the B3LYP/6-311++G(3df,3pd) level. The combined energy of the isolated monomers on the reactant side has been taken as zero at infinite separation.

level, with that reported at the same level of calculation by Ignatov et al.[61] Our B3LYP/6-311++G(3df,3pd) level calculations predict an electronic energy and imaginary frequency for the TS of respectively −777.8823568 hartree and 643*i* cm^{-1}, which are very similar to their reported values (−777.8823413 hartree and 643*i* cm^{-1}) computed at the same level. The small difference (0.0000155 hartree ≡ 0.0097 kcal/mol) in the calculated electronic energies between the two investigations arises because the transition states located by us and Ignatov et al. are near-isoenergetic conformers that differ slightly from each other with respect to the orientations of hydrogen atoms in the TS that are not actively involved in hydrogen bonding. Such nearly isoenergetic conformers of the $SO_3\cdots H_2O\cdots H_2O$ complex and their corresponding transition states, which basically differ from each other with respect to the orientations of the hydrogen atoms that are not involved in hydrogen bonding, have been previously reported by Standard et al.[62] Basically, the exact geometry of the TS that one finds depends on the corresponding initial structure of the $SO_3\cdots H_2O\cdots H_2O$ reactant complex with which one starts the search.[62] The calculations performed by Standard et al.[62] at the MP2/6-311++G(2df,2pd) level show that the difference in binding energies and/or activation barrier heights between two such different conformers is only 0.3 kcal/mol. Therefore, irrespective of the staring conformer for the $SO_3\cdots H_2O\cdots H_2O$ complex, it is seen that the binding energy and barrier height remain very nearly identical with respect to the different orientations of the water molecules; this is also reflected in the same values for the computed imaginary frequencies for the two different transition state structures located in this study and by Ignatov et al.[61] Finally, we compare our results with the work of Morokuma and Muguruma, who were the first to investigate the SO_3 hydrolysis involving two water molecules.[55] Their ab initio calculations were carried out at the MP4SDQ/6-311+G(d,p)//MP2/6-311+G(d,p)+ZPE(HF/6-311+G(d,p) level (hereafter referred to as MP4SDQ) and predicted an activation energy barrier of ∼13 kcal/mol for the unimolecular isomerization step that converts the $SO_3\cdots H_2O\cdots H_2O$ complex to $H_2SO_4\cdots H_2O$. At the MP4SDQ level, the energies of the $SO_3 + H_2O\cdots H_2O$ and $SO_3\cdots H_2O + H_2O$ reactants were found to be respectively 0.7 and 5.3 kcal/mol lower than that of the transition state. Thus, the main differences between our potential energy diagram and that first reported by Morokuma and Muguruma[55] for the water assisted hydrolysis are (a) that the barrier height for the unimolecular isomerization of the $SO_3\cdots H_2O\cdots H_2O$ complex is substantially lower than that predicted by Morokuma and Muguruma and (b) that there is a different energetic position of the TS with respect to the energies of the $SO_3 + H_2O\cdots H_2O$ as well as the $SO_3\cdots H_2O + H_2O$ reactants. In our calculations, the barrier height for the rate determining step involving unimolecular isomerization of the $SO_3\cdots H_2O\cdots H_2O$ complex is computed to be 7.05 and 6.53 kcal/mol, respectively, at the B3LYP/6-311++G(3df,3pd) and MP2/6-311++G(3df,3pd) levels. Our value is consistent with the results of Standard et al., who report a barrier height between 6.6 and 6.7 kcal/mol for the $SO_3\cdots H_2O\cdots H_2O$ isomerization step at the MP2/6-311++G(2df,2pd) level.[62] Furthermore, as shown in Figure 5, we find that the zero point vibrational energy corrected total energies for the $SO_3 + H_2O\cdots H_2O$ and $SO_3\cdots H_2O + H_2O$ reactants are predicted to be respectively 6.48 and 2.37 kcal/mol higher than the energy of the TS at the MP2/6-311++G(3df,3pd) level (see Table 1 of the Supporting Information). The ab initio calculation by other groups[58−62] on this system at the MP2, B3LYP, and CCSD(T) levels using various medium to large basis sets also finds a substantially lower barrier height for the unimolecular isomerization step and a different positioning of the reactant energies relative to the TS compared to that found in the early work of Morokuma and Muguruma using the MP4SDQ level calculations. Thus, the energetics reported for this reaction depends on the size of the basis, and based on the above discussion, we conclude that our results for the water assisted SO_3 hydrolysis are consistent with the most recent studies using the larger basis sets.

Next, we directly compare the energetics of the FA and water assisted unimolecular isomerization reactions. The most important difference between these two hydrolysis reactions is that in the case of FA the unimolecular isomerization of the prereactive $SO_3\cdots H_2O\cdots$FA complex, whether it is formed from $SO_3\cdots H_2O$ + FA or SO_3 + FA$\cdots H_2O$ as reactant, is effectively a barrierless process for producing $H_2SO_4\cdots H_2O$. This energetic difference in the barrier heights is highlighted in Figure 6, where the two reactions are compared after taking the energies of the

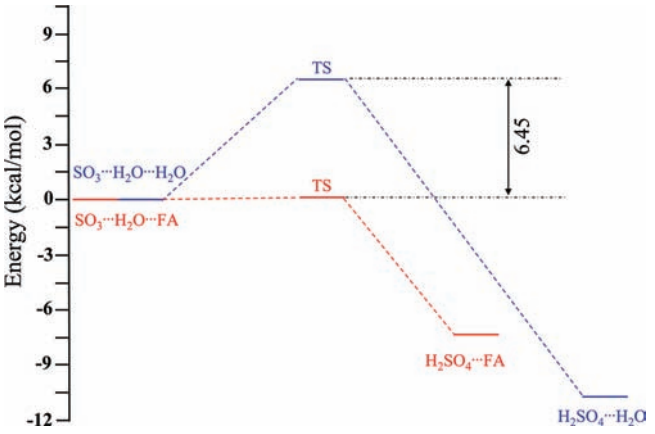

Figure 6. Zero point vibrational energy (ZPE) corrected energy difference for the activation barriers in the water and formic acid (FA) assisted unimolecular isomerization reactions predicted at the MP2/6-311++G-(3df,3pd) level. The ZPE corrected energies of $SO_3\cdots H_2O\cdots H_2O$ and $SO_3\cdots H_2O\cdots FA$ complexes have been taken as zero.

$SO_3\cdots H_2O\cdots H_2O$ and $SO_3\cdots H_2O\cdots FA$ prereactive complexes to a common energy origin. As Figure 6 shows, at the MP2/6-311++G(3df,3pd) level, the barrier height for the water assisted hydrolysis is 6.45 kcal/mol higher than that for the FA assisted reaction. Interestingly, the B3LYP/6-311++G(3df,3pd) calculation also gives a similar difference in the barrier height and suggests that the barrier for water assisted hydrolysis is 6.46 kcal/mol higher than that for formic acid.

3B. Relative Rates and Potential Atmospheric Impact. Given the ability of FA to lower the barrier for SO_3 hydrolysis, it can potentially play an important role in the formation of atmospheric H_2SO_4 and, hence, aerosols. It is useful to examine the possible atmospheric impact of the FA assisted hydrolysis by comparing its rate relative to that for the water assisted reaction, which we use as a reference. We point out that it is not the goal of the present work to calculate absolute rates but to only examine relative rates associated with reagent energetics computed at the same level of theory. We first consider the kinetic expression associated with the water assisted reaction, which, as noted earlier, can proceed via two pathways: one involving the $SO_3\cdots H_2O + H_2O$ reactants and the other involving the water dimer, via $SO_3 + H_2O\cdots H_2O$. These paths are difficult to distinguish experimentally, as they are both second order with respect to the water concentration, and to the best of our knowledge there has been no prior analysis in the literature addressing whether one of the pathways dominates over the other. Consequently, we examine this aspect of the water assisted reaction first. For the $SO_3\cdots H_2O + H_2O$ pathway, the main steps are as follows:

$$SO_3 + H_2O \rightleftharpoons SO_3\cdots H_2O \quad (7)$$

$$SO_3\cdots H_2O + H_2O \rightleftharpoons SO_3\cdots H_2O\cdots H_2O \quad (8)$$

$$SO_3\cdots H_2O\cdots H_2O \rightarrow H_2SO_4\cdots H_2O \quad (9)$$

As already noted, the above reaction sequence is typically viewed as one involving the formation of the $SO_3\cdots H_2O\cdots H_2O$ prereactive collision complex, which then undergoes unimolecular isomerization. Applying a steady state approximation to this prereactive collision complex and assuming that it is in equilibrium with the reactants, the rate law for the formation of H_2SO_4 has been expressed in the literature as[63]

$$\left[\frac{d[H_2SO_4]}{dt}\right] = \text{rate}_{\text{water-monomer}} = K_{SO_3\,-\,H_2O}\frac{k_8}{k_{-8}}k_9[H_2O]^2[SO_3] \quad (10)$$

The above rate equation expresses the fact that formation of H_2SO_4 in the gas phase is second order with respect to water concentration and first order with respect to SO_3 concentration.[40,49,50] In the above equation, $K_{SO_3-H_2O}$ is the equilibrium constant for the formation of the starting $SO_3\cdots H_2O$ reactant complex from isolated SO_3 and H_2O and k_i/k_{-i} denote the forward and reverse rate coefficients for the i-th reaction step. For the SO_3 hydrolysis pathway involving a water dimer ($H_2O\cdots H_2O$), the steps are similar and consist of the following:

$$H_2O + H_2O \rightleftharpoons H_2O\cdots H_2O \quad (11)$$

$$SO_3 + H_2O\cdots H_2O \rightleftharpoons SO_3\cdots H_2O\cdots H_2O \quad (12)$$

$$SO_3\cdots H_2O\cdots H_2O \rightarrow H_2SO_4\cdots H_2O \quad (13)$$

The above reaction sequence gives rise to a rate expression for sulfuric acid formation analogous to eq 10:

$$\left[\frac{d[H_2SO_4]}{dt}\right]_{\text{water-dimer}} = \text{rate}_{\text{water-dimer}} = K_{H_2O\,-\,H_2O}\frac{k_{12}}{k_{-12}}k_{13}[H_2O]^2[SO_3] \quad (14)$$

Additionally, in eqs 10 and 14, the ratio of the forward and reverse rate coefficients for reaction steps 8 and 12 for the formation and decomposition of the $SO_3\cdots H_2O\cdots H_2O$ prereactive complex from their respective reactants, the terms k_8/k_{-8} and k_{12}/k_{-12}, can be expressed as equilibrium constants denoted respectively as K'_8 and K'_{12}. As a result, the ratio of the two rate expressions in eqs 10 and 14 can be written compactly as follows:

$$\frac{\text{rate}_{\text{water-dimer}}}{\text{rate}_{\text{water-monomer}}} = \frac{K_{H_2O\,-\,H_2O}}{K_{SO_3\,-\,H_2O}}\frac{K'_{12}}{K'_8}\frac{k_{13}}{k_9} \quad (15)$$

Using ab initio values for vibrational frequencies, rotational constants, and binding energies, given in the Supporting Information, the required equilibrium constants for the reactant complex and prereactive collision complex can be determined from statistical thermodynamics.[83] Furthermore, the rates for the unimolecular isomerization of the $SO_3\cdots H_2O\cdots H_2O$ prereactive complex (k_{13} and k_9) can be estimated using simple microcanonical RRKM theory.[84] The energized prereactive complexes formed via the two pathways, one involving the water dimer and the other involving the water monomer, have different energies but share a common transition state.[55] At the MP2/6-311++G(3df,3pd) level, we find that the $SO_3\cdots H_2O\cdots H_2O$ prereactive complex has 4.11 kcal/mol more energy (including zero point corrections) when formed from the water dimer channel (i.e., $SO_3 + H_2O\cdots H_2O$) versus the monomer pathway (i.e., $SO_3\cdots H_2O + H_2O$). The sum and density of states for the reactants and transition state, required for the RRKM calculation, were computed using the Whitten−Rabinovitch procedure as outlined in ref 84. Our calculations show that SO_3 hydrolysis via the $SO_3 + H_2O\cdots H_2O$ pathway is approximately 10 times faster

relative to the pathway involving the $SO_3\cdots H_2O + H_2O$ reactants. Thus, as shown in Figure 5, although $SO_3\cdots H_2O$ is more stable compared to the $H_2O\cdots H_2O$ dimer, the higher excess energy (~4.11 kcal/mol) in the $SO_3\cdots H_2O\cdots H_2O$ complex when it is formed through the $SO_3 + H_2O\cdots H_2O$ pathway drives the reaction toward product faster compared to when the same complex is formed through the $SO_3\cdots H_2O + H_2O$ reactants. Given the apparent dominance of the water dimer pathway in the water assisted hydrolysis of SO_3, we next compare the rate of the FA assisted reaction with that for the water dimer channel. The sequence of steps for the FA assisted reaction is similar to that discussed above for water and involves the following steps:

$$SO_3 + H_2O \rightleftharpoons SO_3\cdots H_2O \quad (16)$$

$$SO_3\cdots H_2O + FA \rightleftharpoons SO_3\cdots H_2O\cdots FA \quad (17)$$

$$SO_3\cdots H_2O\cdots FA \rightarrow H_2SO_4\cdots FA \quad (18)$$

If we apply a kinetic analysis to the FA-assisted mechanism that is similar to that applied to water, the following rate expression results:

$$\left[\frac{d[H_2SO_4]}{dt}\right]_{FA\text{-assisted}} = \text{rate}_{FA\text{-assisted}} = K_{SO_3\,-\,H_2O}\frac{k_{17}}{k_{-17}}\,k_{18}[H_2O][FA][SO_3] \quad (19)$$

As in the case of the water assisted reaction, we express the ratio of the rates k_{17}/k_{-17} for the formation and decomposition of the $SO_3\cdots H_2O\cdots FA$ prereactive complex from its starting reactants as an equilibrium constant denoted by K'_{17}. Then taking the ratio of the two rate expressions given in eqs 14 and 19, we get that

$$\frac{\text{rate}_{FA\text{-assisted}}}{\text{rate}_{water-dimer}} = \frac{K_{SO_3\,-\,H_2O}}{K_{H_2O\,-\,H_2O}}\frac{K'_{17}}{K'_{12}}\frac{k_{18}}{k_{13}}\frac{[FA]}{[H_2O]} \quad (20)$$

Thus, the analysis of the relative rates reduces to investigating the contributions from the four ratios appearing in eq 20. In the region of the middle troposphere, the concentration of water vapor is larger than that of FA by roughly 5 orders of magnitude,[67,68,71,85−88] resulting in the contribution from the concentration ratio in eq 20 being $\sim 10^{-5}$. The ratio of the rate constants (k_{18}/k_{13}) for the unimolecular isomerization steps is obtained by applying microcanonical RRKM theory.[84] For the RRKM calculations (see the Supporting Information) we assume that the internal energy of the prereactive collision complex, either $SO_3\cdots H_2O\cdots H_2O$ or $SO_3\cdots H_2O\cdots FA$, is just the thermal energy ($^3/_2kT$) added to their respective zero point energy corrected binding energy for formation from the appropriate reactants. This energy determines the available energy driving the reactions over the unimolecular isomerization barrier. The RRKM calculations show that, for temperatures in the range 200−300 K, the ratio of the rate constants (k_{18}/k_{13}) is $\sim 10^3$, in favor of the barrierless FA assisted reaction. We point out that the term "barrierless" is used here to indicate a very small barrier and not a situation where the TS is not well-defined, thus requiring the application of variational RRKM theory.[89] As before, the ratio of equilibrium constants (K'_{17}/K'_{12}) can be obtained from the ratio of partition functions and taking into account the appropriate binding energies.[83] In our calculation of the partition functions, we use rotational constants and harmonic vibrational frequencies computed at the B3LYP/6-311++G(3df,3pd) level and zero point energy corrected binding energies computed at the MP2/6-311++G(3df,3pd) level. Using these values, we estimate the ratio of the equilibrium constants (K'_{17}/K'_{12}) in eq 20 to be ~3.5 at 300 K and this ratio increases to ~11.5 at 200 K due to the higher binding energy of the $SO_3\cdots H_2O\cdots FA$ complex relative to the $SO_3\cdots H_2O\cdots H_2O$ complex. Finally, the ratio of the equilibrium constants ($K_{SO_3-H_2O}/K_{H_2O-H_2O}$) ranges between 28 at 300 K and 85 at 200 K. Thus, taken together, the four factors appearing in eq 20 combine to give a ratio of the rates which ranges between ~1 to 10, in favor of the FA catalyzed reaction. Hence, this rather simple relative rate analysis suggests that FA assisted hydrolysis of SO_3 to form H_2SO_4 is very much competitive with, and may even surpass, the rate for the currently accepted scheme involving water assisted hydrolysis in the atmosphere. We note that our present analysis neglects tunneling as well as variation of the rates with atmospheric pressure, which could be treated using a master equation approach such as that performed on other atmospheric reaction systems;[90] however, we defer these refinements for future work. The calculated equilibrium constants and unimolecular isomerization rates required for our kinetics analysis, presented above, are given in the Supporting Information. Finally, we note that although we have considered only the $SO_3\cdots H_2O$ + FA pathway, we expect the rate for the complementary pathway involving the SO_3 + $FA\cdots H_2O$ reactants to be similar. This follows from the fact that both the $SO_3\cdots H_2O$ and $FA\cdots H_2O$ reactant complexes are nearly isoenergetic (see Figure 3) with respect to their binding energies and their reaction involves formation of the same prereactive collision complex and transition state. Thus, both pathways are expected to form the $SO_3\cdots H_2O\cdots FA$ prereactive complex with similar excess energies and, hence, exhibit similar unimolecular isomerization rates.

The above findings have potentially important implications for the chemistry associated with atmospheric aerosol formation. As mentioned earlier, H_2SO_4 abundance in the atmosphere is known to be strongly related to the fundamental step in atmospheric new-particle formation. To date, the basic mechanisms for atmospheric aerosol formation are not yet completely understood and the composition of the "critical nucleus" required for the formation of new aerosol particles has been the subject of intense studies.[11,12,14,91−95] Several studies indicate that the "critical nucleus" for aerosol formation may contain only one molecule of an organic acid.[12,14,91,92,96−100] Recent laboratory experiments and theoretical calculations show that nucleation around sulfuric acid, and hence aerosol growth, is considerably enhanced in the presence of aromatic acids such as benzoic acid, *p*-toluic acid, and *m*-toluic acid.[12] The high binding energies of these sulfuric acid−organic acid complexes apparently lead to reduced nucleation barriers and possibly promote the efficient formation of organic−sulfate aerosols in polluted atmosphere. Studies by Zhang et al.[91] with *cis*-pinonic acid (CPA), for example, suggest that the formation of a sulfuric acid−organic acid H-bonded complex is most likely responsible for a reduction in the nucleation barrier through modification of the hydrophobic properties of the organic acid, thus allowing further addition of hydrophilic species such as H_2SO_4, H_2O, and possibly NH_3 required to propagate aerosol growth. The present computational work shows that the hydrolysis of SO_3, which is the key step in atmospheric sulfuric acid formation, can be effectively catalyzed by just one molecule of FA to form the $H_2SO_4\cdots FA$ complex. Given that the sulfuric acid and organic acid units are already tethered together in this complex as a part of the sulfuric acid formation step, such FA catalyzed SO_3 hydrolysis reactions could then, in principle, provide an efficient first step for

generating the critical nucleus necessary for propagating atmospheric aerosol growth. Further, the present computational results with FA suggest that potential parallel catalytic behavior involving other monocarboxylic acids may also be possible. Hence, more generally, a variety of atmospheric organic acid molecules (OA) or their hydrated complex ($OA\cdots H_2O$) can collide respectively with $SO_3\cdots H_2O$ or SO_3 and thereby catalyze the hydrolysis of SO_3 to form the $OA\cdots H_2SO_4$ complex required for initiating aerosol formation.

4. SUMMARY AND CONCLUSION

The gas phase conversion of SO_3 to H_2SO_4 in the atmosphere is currently believed to occur primarily via the $SO_3 + 2H_2O$ reaction with the second water molecule acting as a catalyst. Quantum chemistry calculations show that the rate determining step for this reaction is the unimolecular isomerization of the $SO_3\cdots H_2O\cdots H_2O$ prereactive collision complex to give $H_2SO_4\cdots H_2O$. In the atmosphere, there is a substantial abundance of formic acid (FA), and therefore, analogous to the situation associated with water assisted hydrolysis of SO_3, the tertiary $SO_3\cdots H_2O\cdots FA$ prereactive complex can form through either of two pathways involving $SO_3\cdots H_2O$ + FA and/or SO_3 + $FA\cdots H_2O$. Our calculations show that, once formed, the $SO_3\cdots H_2O\cdots FA$ complex can undergo facile unimolecular isomerization to produce $H_2SO_4\cdots FA$ and finally sulfuric acid. Calculations show that the FA assisted hydrolysis of SO_3 is effectively a barrierless process with the barrier height for the rate determining unimolecular isomerization step being only 0.59 and 0.08 kcal/mol, respectively, at the B3LYP/6-311++G(3df,3pd) and MP2/6-311++G(3df,3pd) levels. The corresponding barrier heights for the water assisted unimolecular isomerization step are respectively 7.05 and 6.53 kcal/mol at the same levels. A simple comparison of the relative rate expressions for the two hydrolysis mechanisms suggests that FA assisted hydrolysis of SO_3 to form H_2SO_4 is very much competitive with, and may even surpass, the rate for the currently accepted scheme involving water assisted hydrolysis. Thus, the new mechanism can impact our understanding of atmospheric sulfuric acid formation and, hence, the rate of aerosol production in the Earth's atmosphere.[95] The current results also suggest that inclusion of an organic acid (OA) into sulfuric acid aerosol, often seen from analysis of atmospheric aerosol composition,[12,14] may occur prior to the formation of the sulfuric acid itself, as the organic acid provides a facile route for the hydrolysis of SO_3 and eventual formation of the stabilized $H_2SO_4\cdots OA$ dimer via the $SO_3\cdots H_2O\cdots OA$ prereactive collision complex.

■ ASSOCIATED CONTENT

Supporting Information. Complete refs 77 and 95, calculated electronic energies for monomers and complexes, the MP2/6-311++G(3df,3pd) level optimized geometries of $SO_3\cdots H_2O\cdots FA$, $H_2SO_4\cdots FA$, and TS located in the $SO_3\cdots H_2O\cdots FA \rightarrow H_2SO_4\cdots FA$ unimolecular isomerization step, the two starting initial geometries of the $SO_3\cdots H_2O\cdots FA$ complex as has been discussed in the text, and rotational constants, vibrational frequencies, equilibrium constants, and RRKM unimolecular isomerization rates as required for kinetic analysis. This material is available free of charge via the Internet at http://pubs.acs.org.

■ AUTHOR INFORMATION

Corresponding Author
asinha@ucsd.edu

■ ACKNOWLEDGMENT

We thank the National Science Foundation for the support of this work.

■ REFERENCES

(1) Pruppacher, H. R; Klett, J. D. *Microphysics of Clouds and Precipitation*; Reidel: Dordrecht, 1980.
(2) Stockwell, W. R.; Calvert, J. G. *Atmos. Environ.* **1983**, *17*, 2231.
(3) Finlayson-Pitts, B. J.; Pitts, J. N., Jr. *Atmospheric Chemistry*; Wiley: New York, 1986.
(4) Weber, R. J.; McMurry, P. H.; Eisele, F. L.; Tanner, D. J. *J. Atmos. Sci.* **1995**, *52*, 2242.
(5) Weber, R. J.; Marti, J. J.; McMurry, P. H.; Eisele, F. L.; Tanner, D. J.; Jefferson, A. *Chem. Eng. Commun.* **1996**, *151*, 53.
(6) Weber, R. J.; Chen, G.; Davis, D. D.; Mauldin, R. L., III; Tanner, D. J.; Eisele, F. L.; Clarke, A. D.; Thornton, D. C.; Bandy, A. R. *J. Geophys. Res.* **2001**, *106*, 24107.
(7) Sihto, S.-L.; Kulmala, M.; Kerminen, V.-M.; Dal Maso, M.; Petäjä, T.; Riipinen, I.; Korhonen, H.; Arnold, F.; Janson, R.; Boy, M.; Laaksonen, A.; Lehtinen, K. E. J. *Atmos. Chem. Phys.* **2006**, *6*, 4079.
(8) Riipinen, I.; Sihto, S.-L.; Kulmala, M.; Arnold, F.; Dal Maso, M.; Birmili, W.; Saarnio, K.; Teinilä, K.; Kerminen, V.-M.; Laaksonen, A.; Lehtinen, K. E. J. *Atmos. Chem. Phys.* **2007**, *7*, 1899.
(9) Kuang, C.; McMurry, P. H.; McCormick, A. V.; Eisele, F. L. *J. Geophys. Res.* **2008**, *113*, D10209.
(10) Sipilä, M.; Berndt, T.; Petäjä, T.; Brus, D.; Vanhanen, J.; Stratmann, F.; Patokoski, J.; Mauldin, R. L., III; Hyvärinen, A.-P.; Lihavainen, H.; Kulmala, M. *Science* **2010**, *327*, 1243.
(11) Kulmala, M.; Pirjola, L.; Mäkelä, J. M. *Nature* **2000**, *404*, 66.
(12) Zhang, R.; Suh, I.; Zhao, J.; Zhang, D.; Fortner, E. C.; Tie, X.; Molina, L. T.; Molina, M. J. *Science* **2004**, *304*, 1487.
(13) Lovejoy, E. R.; Curtius, J.; Froyd, K. D. *J. Geophys. Res.* **2004**, *109*, D08204.
(14) Zhang, R. *Science* **2010**, *328*, 1366.
(15) Finlayson-Pitts, B. J.; Pitts, J. N., Jr. *Chemistry of the Upper and Lower Atmosphere: Theory, Experiments, and Applications*; Academic Press: San Diego, CA, 2000.
(16) Seinfeld, J. H.; Pandis, S. N. *Atmospheric Chemistry and Physics: From Air Pollution to Climate Change*; Wiley: New York, 1998.
(17) Charlson, R. J.; Lovelock, J. E.; Andreae, M. O.; Warren, S. G. *Nature* **1987**, *326*, 655.
(18) Houghton, J. T., Ding, Y., Griggs, D. J., Noguer, M., van der Linden, P. J., Dai, X., Maskell, K., Johnson, C. A., Eds. *Climate Change 2001: The Scientific Basis*; Cambridge University Press: Cambridge, 2001.
(19) Orville, R. E.; Huffines, G.; Nielsen-Gammon, J.; Zhang, R.; Ely, B.; Steiger, S.; Phillips, S.; Allen, S.; Read, W. *Geophys. Res. Lett.* **2001**, *28*, 2597.
(20) Zhang, R.; Tie, X.; Bond, D. W. *Proc. Natl. Acad. Sci. U.S.A.* **2003**, *100*, 1505.
(21) Vaida, V.; Kjaergaard, H. G.; Hintze, P. E.; Donaldson, D. J. *Science* **2003**, *299*, 1556.
(22) Miller, Y.; Gerber, R. B.; Vaida, V. *Geophys. Res. Lett.* **2007**, *34*, L16820.
(23) Govoni, S. T.; Nathanson, G. M. *J. Am. Chem. Soc.* **1994**, *116*, 779.
(24) Nathanson, G. M. *Annu. Rev. Phys. Chem.* **2004**, *55*, 231.
(25) Hintze, P. E.; Kjaergaard, H. G.; Vaida, V.; Burkholder, J. B. *J. Phys. Chem. A* **2003**, *107*, 1112.
(26) Givan, A.; Larsen, L. A.; Loewenschuss, A.; Nielsen, C. J. *J. Mol. Struct.* **1999**, *509*, 35.

(27) Feierabend, K. J.; Havey, D. K.; Brown, S. S.; Vaida, V. *Chem. Phys. Lett.* **2006**, *420*, 438.
(28) Hintze, P. E.; Feierabend, K. J.; Havey, D. K.; Vaida, V. *Spectrochim. Acta A* **2005**, *61*, 559.
(29) Burkholder, J. B.; Mills, M.; McKeen, S. *Geophys. Res. Lett.* **2000**, *27*, 2493.
(30) Bell, R. M.; Jeppesen, M. A. *J. Chem. Phys.* **1935**, *3*, 245.
(31) Radüge, C.; Pflumio, V.; Shen, Y. R. *Chem. Phys. Lett.* **1997**, *274*, 140.
(32) Fiacco, D. L.; Hunt, S. W.; Leopold, K. R. *J. Am. Chem. Soc.* **2002**, *124*, 4504.
(33) Havey, D. K.; Feierabend, K. J.; Vaida, V. *THEOCHEM* **2004**, *680*, 243.
(34) Nash, K. L.; Sully, K. J.; Horn, A. B. *Phys. Chem. Chem. Phys.* **2000**, *2*, 4933.
(35) Wrenn, S. J.; Butler, L. J.; Rowland, G. A.; Knox, C. J. H.; Phillips, L. F. *J. Photochem. Photobiol. A: Chem.* **1999**, *129*, 101.
(36) Robinson, T. W.; Schofield, D. P.; Kjaergaard, H. G. *J. Chem. Phys.* **2003**, *118*, 7226.
(37) Miller, Y.; Chaban, G. M.; Gerber, R. B. *J. Phys. Chem. A* **2005**, *109*, 6565.
(38) Latimer, W. T.; Hildenbrand, J. L. *Reference Book of Inorganic Chemistry*; Macmillan Co.: New York, 1929.
(39) Castleman, A. W.; Davis, R. E.; Munkelwitz, H. R.; Tang, I. N.; Wood, W. P. *Int. J. Chem. Kinet. Symp.* **1975**, *1*, 629.
(40) Kolb, C. E.; Jayne, J. T.; Worsnop, D. R.; Molina, M. J.; Meads, R. F.; Viggiano, A. A. *J. Am. Chem. Soc.* **1994**, *116*, 10314.
(41) Goodeve, C. F.; Eastman, A. S.; Dooley, A. *Trans. Faraday Soc.* **1934**, *30*, 1127.
(42) Hofmann-Sievert, R.; Castleman, A. W., Jr. *J. Phys. Chem.* **1984**, *88*, 3329.
(43) Chen, T. S.; Moore-Plummer, P. L. *J. Phys. Chem.* **1985**, *89*, 3689.
(44) Bondeybey, V. E.; English, J. H. *J. Mol. Spectrosc.* **1985**, *109*, 221.
(45) Wang, X.; Jin, Y. G.; Suto, M.; Lee, L. C. *J. Chem. Phys.* **1988**, *89*, 4853.
(46) Reiner, T. H.; Arnold, F. *Geophys. Res. Lett.* **1993**, *20*, 2659.
(47) Reiner, T. H.; Arnold, F. *J. Chem. Phys.* **1994**, *101*, 7399.
(48) Phillips, J. A.; Canagaratna, M.; Goodfriend, H.; Leopold, K. R. *J. Phys. Chem.* **1995**, *99*, 501.
(49) Lovejoy, E. R.; Hanson, D. R.; Huey, G. *J. Phys. Chem.* **1996**, *100*, 19911.
(50) Jayne, J. T.; Pöschl, U.; Chen, Y.-N.; Dai, D.; Molina, L. T.; Worsnop, D. R.; Kolb, C. E.; Molina, M. J. *J. Phys. Chem.* **1997**, *101*, 10000.
(51) Akhmatskaya, E. V.; Apps, C. J.; Hillier, I. H.; Masters, A. J.; Watt, N. E.; Whitehead, J. C. *J. Chem. Soc., Faraday Trans.* **1997**, *93*, 2775.
(52) Holland, P. M.; Castleman, A. W., Jr. *Chem. Phys. Lett.* **1978**, *56*, 511.
(53) Chen, T. S.; Moore-Plummer, P. L. *J. Phys. Chem.* **1985**, *89*, 3689.
(54) Hofmann, M.; Schleyer, P. v. R. *J. Am. Chem. Soc.* **1994**, *116*, 4947.
(55) Morokuma, K.; Murguruma, C. *J. Am. Chem. Soc.* **1994**, *116*, 10316.
(56) Steudel, R. *Angew. Chem., Ind. Ed.* **1995**, *34*, 1313.
(57) Meijer, E. J.; Sprik, M. *J. Phys. Chem. A* **1998**, *102*, 2893.
(58) Larson, L. J.; Kuno, M.; Tao, F.-M. *J. Chem. Phys.* **2000**, *112*, 8830.
(59) Loerting, T.; Liedl, K. R. *Proc. Natl. Acad. Sci. U.S.A.* **2000**, *97*, 8874.
(60) Loerting, T.; Liedl, K. R. *J. Phys. Chem. A* **2001**, *105*, 5137.
(61) Ignatov, S. K.; Sennikov, P. G.; Razuvaev, A. G.; Schrems, O. *J. Phys. Chem. A* **2004**, *108*, 3642.
(62) Standered, J. M.; Buckner, I. S.; Pulsifer, D. H. *THEOCHEM* **2004**, *673*, 1.
(63) Fliegl, H.; Glöβ, A.; Welz, O.; Olzmann, M.; Klopper, W. *J. Chem. Phys.* **2006**, *125*, 054312.
(64) Gonzalez, J.; Torrent-Sucarrat, M.; Anglada, J. M. *Phys. Chem. Chem. Phys.* **2010**, *12*, 2116.
(65) Kawamura, K.; Kaplan, I. R. *Environ. Sci. Technol.* **1983**, *17*, 497.
(66) Kawamura, K.; Kaplan, I. R. *Anal. Chem.* **1984**, *56*, 1616.
(67) Grosjean, D. *Environ. Sci. Technol.* **1989**, *23*, 1506.
(68) Shephard, M. W.; Goldman, A.; Clough, S. A.; Mlawer, E. J. *J. Quant. Spectrosc. Radiat. Transfer* **2003**, *82*, 383.
(69) Rinsland, C. P.; Mahieu, E.; Zander, R.; Goldman, A.; Wood, S.; Chiou, L. *J. Geophys. Res.* **2004**, *109*, D18308.
(70) Abad, G. G.; Bernath, P. F.; Boone, C. D.; McLeod, S. D.; Manney, G. L.; Toon, G. C. *Atoms. Chem. Phys.* **2009**, *9*, 8039.
(71) Grutter, M.; Glatthor, N.; Stiller, G. P.; Fischer, H.; Grabowski, U.; Höpfner, M.; Kellmann, S.; Linden, A.; von Clarmann, T. *J. Geophys. Res.* **2010**, *115*, D10303.
(72) Hazra, M. K.; Chakraborty, T. *J. Phys. Chem. A* **2005**, *109*, 7621.
(73) Hazra, M. K.; Chakraborty, T. *J. Phys. Chem. A* **2006**, *110*, 9130.
(74) Buszek, R. J.; Sinha, A.; Francisco, J. S. *J. Am. Chem. Soc.* **2011**, *133*, 2013.
(75) da Silva, G. *Angew. Chem., Ind. Ed.* **2010**, *49*, 7523.
(76) Maeda, S.; Komagawa, S.; Uchiyama, M.; Morokuma, K. *Angew. Chem., Ind. Ed.* **2011**, *50*, 644.
(77) Frisch, M. J.; et al. *GAUSSIAN 03*, Revision B.04; Gaussian Inc.: Pittsburgh, PA, 2003.
(78) Lee, C.; Yang, W.; Parr, R. G. *Phys. Rev. B* **1988**, *37*, 785.
(79) Becke, A. M. *J. Chem. Phys.* **1993**, *98*, 5648.
(80) Reimann, B.; Buchhold, K.; Barth, H.-D.; Brutschy, B.; Tarakeshwar, P.; Kim, K. S. *J. Chem. Phys.* **2002**, *117*, 8805.
(81) Alvarez-Idaboy, J. R.; Galano, A. *Theor. Chem. Acc.* **2010**, *126*, 75.
(82) Galano, A.; Alvarez-Idaboy, J. R. *J. Comput. Chem.* **2006**, *27*, 1203.
(83) McQuarrie, D. A. *Statistical Thermodynamics*; Harper and Row: New York, 1973.
(84) Steinfeld, J. I.; Francisco, J. S.; Hase, W. L. *Chemical Kinetics and Dynamics*, 2nd ed.; p 345.
(85) DeMore, W. B.; Sander, S. P.; Golden, D. M.; Hampson, R. F.; Kurylo, M. J.; Howard, C. J.; Ravishankara, A. R.; Kolb, C. E.; Molina, M. J. *Chemical Kinetics and Photochemical Data for Use in Stratospheric Modeling*, Evaluation Number 12; JPL Publication 97-4; Jet Propulsion Laboratory, California Institute of Technology: Pasadena, CA, 1997.
(86) Legrand, M.; de Angelis, M. *J. Geophys. Res.* **1995**, *100*, 1445.
(87) Kesselmeier, J. *J. Atmos. Chem.* **2001**, *39*, 219.
(88) Iuga, C.; Alvarez-Idaboy, J. R.; Vivier-Bunge, A. *J. Phys. Chem. A* **2011**, *115*, 5138.
(89) Hase, W. L. *Acc. Chem. Res.* **1983**, *16*, 258.
(90) Zhang, D.; Zhang, R.; Park, J.; North, S. W. *J. Am. Chem. Soc.* **2002**, *124*, 9600.
(91) Zhao, J.; Khalizov, A. F.; Zhang, R.; McGraw, R. *J. Phys. Chem. A* **2009**, *113*, 680.
(92) Zhang, R.; Wang, L.; Khalizov, A. F.; Zhao, J.; Zheng, J.; McGraw, R. L.; Molina, L. T. *Proc. Natl. Acad. Sci. U.S.A.* **2009**, *106*, 17650.
(93) Schrader, W. *Angew. Chem., Int. Ed.* **2005**, *44*, 1444.
(94) Wang, L.; Khalizov, A. F.; Zheng, J.; Xu, W.; Ma, Y.; Lal, V.; Zhang, R. *Nature Geosci.* **2010**, *3*, 238.
(95) Kirkby, J.; et al. *Nature* **2011**, *476*, 429.
(96) Hoffmann, T.; Bandur, R.; Marggraf, U.; Linscheid, M. *J. Geophys. Res.* **1998**, *103*, 25569.
(97) Kückelmann, U.; Warscheid, B.; Hoffmann, T. *Anal. Chem.* **2000**, *72*, 1905.
(98) Smith, J. N.; Dunn, M. J.; VanReken, T. M.; Iida, K.; Stolzenburg, M. R.; McMurry, P. H.; Huey, L. G. *Geophys. Res. Lett.* **2008**, *35*, L04808.
(99) O'Dowd, C. D.; Aalto, P.; Hämeri, K.; Kulmala, M.; Hoffmann, T. *Nature* **2002**, *416*, 497.
(100) Metzger, A.; Verheggen, B.; Dommen, J.; Duplissy, J.; Prevot, A. S. H.; Weingartner, E.; Riipinen, I.; Kulmala, M.; Spracklen, D. V.; Carslaw, K. S.; Baltensperger, U. *Proc. Natl. Acad. Sci. U.S.A.* **2010**, *107*, 6646.